PHYSICAL REVIEW B VOLUME 49, NUMBER 4 15 JANUARY 1994-II

Strain relief at hexagonal-close-packed interfaces

Harald Brune, Holger Röder, Corrado Boragno, and Klaus Kern
Institut de Physique Expérimentale, EPF Lausanne, CH-1015 Lausanne, Switzerland
(Received 12 October 1993)

The mechanism of strain relief for compressively stressed Ag layers epitaxially grown on Pt(111) is studied by scanning tunneling microscopy. The strain in the compressed commensurate (1×1) Ag monolayer on Pt(111) is relieved in the bilayer by the formation of two weakly incommensurate structures: the metastable striped incommensurate phase, which converts into a trigonal network of domain walls upon annealing. This network is a general case for isotropic strain relief realized by the crossing of domain walls. The introduction of a phase shift of one set of domain walls allows the system to account for the energy difference of fcc and hcp stacking. The stability of unidirectional via isotropic strain relief and the respective structures of domain walls is generally discussed for surface reconstructions and metal epitaxy of hexagonal-close-packed surfaces.

Adsorbed layers on single-crystal surfaces generally are strained due to their lattice mismatch with the substrate. These layers are commensurate (*C*) when the corrugation of the substrate potential acting on the adsorbed atoms is dominating their lateral interaction potential. If the latter is dominant, an incommensurate (*I*) layer results. In this case the adlayer lattice forms moiré patterns with the substrate lattice, which might be rotated to minimize their energy.[1] For the intermediate case, i.e., when both interaction potentials become comparable, weakly incommensurate phases are observed. They consist of large areas which are nearly commensurate, separated by relatively narrow domain walls or discommensurations, where the strain resulting from the lattice mismatch is locally relieved.

Typical candidates for weakly incommensurate phases are metal-on-metal systems (with small lattice mismatch) or reconstructed close-packed metal surfaces, which are, as far as is known, the (111)-oriented surfaces of Au (Refs. 2 and 3) and Pt.[4,5] These reconstructions are driven by the considerable tensile stress in the outermost layer; they consist in the introduction of a certain density of dense domain walls between alternating fcc and hcp stacking regions. For Au(111) the 4% compression of the first layer is achieved by two domain walls per ($\sqrt{3}\times 22$) unit cell, each inserting one-half extra atom, thus leading to 23 atoms adsorbed on 22 second-layer atoms along the close-packed [$1\bar{1}0$] direction.[6,7] Due to the difference in energy more fcc than hcp sites are populated, giving rise to a pairwise arrangement of the [$11\bar{2}$]-oriented domain walls. Locally the compression is unidirectional, however on bigger terraces a mesoscopic order of the domain walls is established: The domain walls bend by ±120° with a period of 250 Å (Ref. 7) forming the so-called herringbone structure which reduces the anisotropy of the surface stress tensor.[8]

In this paper we report on structural manifestations of strain relief in heteroepitaxy of silver on the (111) surface of platinum. The first monolayer (ML) grows in a (1×1) fashion and therefore is isotropically compressed by 8.9% in density with respect to the Ag(111) bulk plane.[9,10] This strain is relieved in the second Ag layer in a metastable unidirectional phase [striped incommensurate (SI)] similar to Au(111) and the behavior observed for Cu on Ru(0001).[11] In contrast to Au(111) and for the second monolayer of Cu on Ru, in the present system the domain walls represent areas of locally lower density. Upon annealing, the SI phase transforms into a trigonal network of crossing domain walls, which we call the trigonal incommensurate (TI) phase. This network is an example for an isotropic strain relief exhibiting different areas for fcc and hcp stacking, thus taking account of the energy difference of these two lattice sites. This is realized by shifting one class of domain walls relative to the crossing point of the two others so that crossing of all three domain walls does not occur. This possibility has been disregarded so far and the difference in energy between the two hollow sites has been considered to stabilize unidirectional strain relief.[11,12] Our example, however, shows that whether domain-wall crossing and thus isotropic strain relief occurs or not depends solely on the domain-wall interaction energy λ (Ref. 13) and the energy cost in the crossing area.

The experiments were performed with a variable-temperature scanning tunneling microscope (STM) (Ref. 9) in an ultrahigh-vacuum (UHV) chamber containing facilities for sputtering and structural and chemical characterization of the sample by low-energy electron diffraction (LEED) and Auger-electron spectroscopy (AES), respectively. The Ag films (purity 99.995%) were evaporated with a molecular-beam-epitaxy (MBE) Knudsen cell at a flux of $R = 1.1\times 10^{-3}$ ML/s and a sample temperature of 300–340 K. After evaporation, the sample has been annealed to the temperatures indicated and subsequently imaged again at 300–340 K. The STM images were recorded in the so-called differential mode, which means that instead of recording the absolute tip height at lines of constant tunnel current, the derivative of these lines was recorded. The grey scale, therefore, represents the surface as it appears when illuminated from the left-hand side.

The structure of the second-monolayer Ag film adsorbed on Pt(111) at 340 K is characterized by the STM image [Fig. 1(a)]. The lower left part and a few one-monolayer-deep holes in the upper part of the image still show the first Ag monolayer, which is imaged flat due to

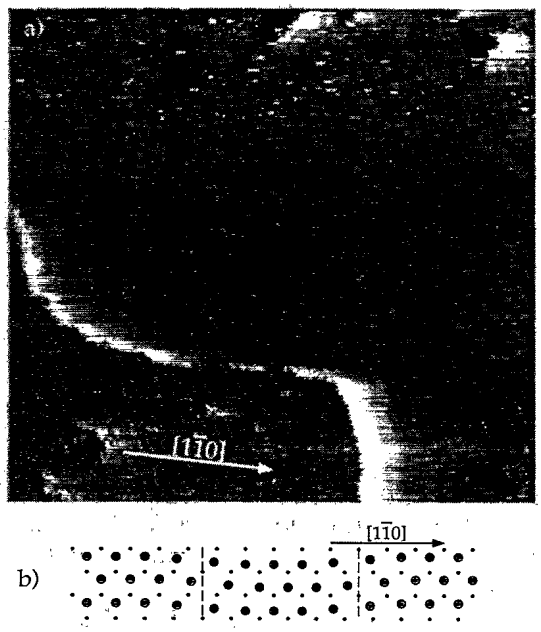

FIG. 1. (a) STM image of the unidirectional relaxed phase obtained at $T=340$ K for the second monolayer Ag on Pt(111) ($\Theta=1.5$ ML, 520×520 Å^2). (b) Atomic model for the striped incommensurate phase [black dots: Ag atoms of the first layer; bright, and dark filled circles: second layer Ag atoms on fcc and hcp positions, respectively].

its (1×1) structure.[9] In contrast, the second-monolayer terrace covering most of the image (the integral coverage is 1.5 ML) reveals two domains of a striped structure rotated by 120°. Localized stripes, imaged dark, are pairwise arranged and separate brighter imaged areas with two different widths. These stripes are running along the [11$\bar{2}$] direction and are bended to U's in the vicinity of the descending Ag step preventing the narrower ones of the bright areas from touching the step. The orientation and the pairwise arrangement as well as the U turns of these stripes are very similar to the domain walls on Au(111).[7] Thus an interpretation of these lines as domain walls separating fcc and hcp stacking regions is straightforward. Those bright areas which face the descending steps have to be attributed to fcc regions because it is reasonable to assume bulk stacking in the vicinity of the steps.[7] In accordance with this interpretation, these areas are bigger by a factor of 2 than those corresponding to the less favorable hcp stacking. The period of this striped phase varies around 37 Å (±3 Å), and can thus be characterized by a $(\sqrt{3}\times p)$ unit cell with $p=(14\pm1)$.

In the known examples of linear incommensurate phases, such as Au(111) and Cu/Ru(0001),[11] the topmost layers are unidirectional compressed relative to the underlying ones, whereas in our case the second Ag layer is unidirectional expanded. A model for the $(\sqrt{3}\times p)$ unit cell therefore consists of $(p-1)$ second-layer atoms adsorbed on p atoms of the first Ag (1×1) layer. At the domain walls the stacking transition from fcc to hcp and vice versa takes place by stretching the Ag-Ag bond along the close-packed direction corresponding to half an atom missing. A model for $p=14$ is shown in Fig. 1(b): eight atoms are adsorbed on fcc sites and five atoms reside on hcp sites, corresponding to an average relaxation by 7.1% along [1$\bar{1}$0]. This decreases the average atomic density close to the Ag(111) value [$\Delta\rho=-8.9\%$ relative to Pt(111)].

The small width of the dark lines in Fig. 1(a) indicates that the domain walls are rather narrow. Hence the dilution of the second Ag layer must be rather localized to the immediate vicinity of the domain walls. To account for this, it has been assumed in the model in Fig. 1(b) that only three Ag-Ag bonds around the domain wall are stretched along [1$\bar{1}$0], and furthermore that most of this stretching is localized to the bond directly at the domain wall. Therefore, the two adjacent atoms to the left and right from the domain wall are shifted only slightly from their hollow position towards each other. Any more homogeneous stretching would result in broader domain walls than the observed one. This rather localized dilution, i.e., one relatively stretched Ag-Ag bond before a more homogeneous distributed strain relief, is energetically favorable for two reasons. First, the disadvantageous bridge sites are not populated in these domain walls. The second argument for a localized stretching of bonds is the asymmetry of the atomic interaction potential around its minimum: For compressed layers one deals with the steep ascending repulsive part of the lateral interaction potential, which makes the layer stiff and rectifies the population of unfavorable sites as bridge and almost on-top sites in U's and stars on Au and Pt(111), respectively.[5,7] However, for diluted layers as in the present case, the soft attractive branch of the potential allows for rather localized stretching of bonds which causes more abrupt changes between the two stacking types.

In Fig. 1(a) and subsequent STM images the domain walls are imaged as depletions of 0.3 Å. Solely from geometric arguments no pronounced variation in height would be expected for the domain walls due to their lack of bridge sites. However, the observed imaging can be understood when the imaging of the first Ag layer is taken into account. Ag (1×1) islands adsorbed on Pt(111) appear in STM images 0.5 Å higher than the geometric height of an Ag(111) plane.[10] This has to be attributed to the 8.9% higher atomic density in a Ag (1×1) layer adsorbed on Pt(111) compared to the Ag(111) plane. This certainly increases also the electronic density and thus the total charge density which is the quantity that determines STM images of metal surfaces to first order.[14] A similarly increased imaging height (0.5 Å) has been observed in STM images of Au on Ru(0001),[15] where the Au (1×1) layer is equally compressed by 6.8%. The imaging of the domain walls as depressions can therefore be understood in terms of their dilution causing a lower electronic density, thus leading to an imaging height close to their geometry, whereas the surrounding areas are imaged higher due to their increased electronic density caused by their compression.

Upon annealing to $T_a=800$ K the SI phase of the second Ag layer converts into a trigonal network of domain walls as demonstrated in Fig. 2(a). The STM image shows two subsequent atomic terraces, both covered with two Ag monolayers. A small area on the right-hand

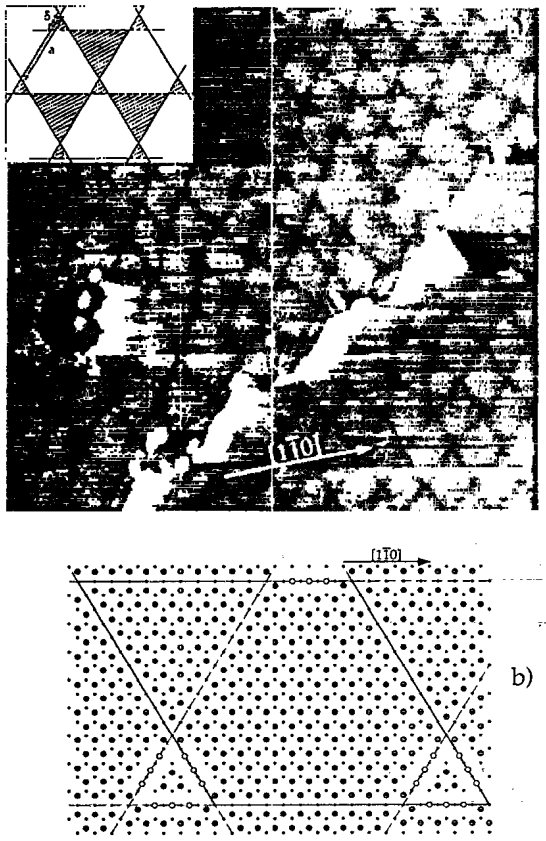

FIG. 2. (a) STM image of the trigonal network constituting the equilibrium structure obtained after annealing of the second Ag monolayer on Pt(111) to $T_a = 800$ K ($\Theta = 1.5$ ML, 520×520 Å^2). Inset: Model for the trigonal network, where domain walls (dark lines) separate fcc and hcp (hatched) areas. (b) Atomic model of the trigonal incommensurate phase [atoms marked equivalent to Fig. 1(b)].

side still shows the commensurate first layer and the position of the former substrate step. On the second layer two almost parallel sets of domain walls rotated by 120° are clearly visible. They are crossing each other enclosing rhombi of slightly elevated imaged areas separated by the again dark imaged domain walls. In addition, each rhombus has a small triangle inscribed on top. Two borders of these triangles consist of the two sets of domain walls; the third borders running almost horizontally are formed by a third set of parallel domain walls. They are clearly visible in the vicinity of these triangles, however they are harder to identify in the areas between adjacent triangles where they are crossing the rhombi. (The lower contrast for the third set of domain walls is due to recording of the $\partial z/\partial x$ signal, which is less sensitive the more parallel features are oriented to the horizontal x.)

In contrast to the SI phase, in the trigonal network the domain walls are oriented along the close-packed [1$\bar{1}$0] direction. A model for this TI phase is shown in the inset of Fig. 2(a). Contrary to the SI phase, the domain walls do cross now, which allows for a more isotropic strain relief. However, the crossing of the three classes of parallel domain walls does not occur in one point, i.e., one set has an offset δ with respect to the crossing point of the other two sets. This generates the small triangles characterizing the structure in Fig. 2(a) and allows for a higher amount of fcc than hcp stacking. The measured value for the offset δ is 0.3 times the period of the network. As is evident from Fig. 2(a), the network is not very regular and reveals many defects. The average period as deduced from STM is (44.8±1.4) Å; it thus can approximately be described by a (16×16) unit cell.

An atomic model for the trigonal structure is shown in Fig. 2(b). Inside one unit cell there are a smaller and a bigger triangle, both of which are hcp stacked, and a fcc stacked hexagon with three longer and three shorter borders. The borders are formed by the [1$\bar{1}$0]-oriented domain walls. Resulting from symmetry there are two different types for these domain walls. The longer borders of the hexagon which incline also the bigger triangles are simply stacking transitions from ideal fcc to hcp positions. The Ag atoms at the domain wall have only five bonds; the one which crosses the domain wall is stretched by 15%. In the shorter type borders, inclining the small triangles and forming the three shorter borders of the hexagons, the atoms populate bridge sites. It is evident that the latter type of domain wall reveals a higher dilution (bonds are stretched by 26%). Hence, due to the total charge-density argument above, it should be imaged lower than the first type, which is indeed found in Fig. 2(a). (The higher geometry of the bridge site is assumed to be overbalanced by the charge-density effect.)

In agreement with the present STM data, the threefold symmetry of the annealed second layer has also been seen in helium diffraction measurements.[16] It results from the unequal size of the two hcp stacked triangles and from the stacking transitions inside the unit cell. According to the atomic model in Fig. 2(b), the density of the second layer is reduced by 7.0%, i.e., 238 second-layer atoms are adsorbed on 256 atoms of the first layer. The ratio of fcc to hcp sites is 2.8, which lies in between the value of 2.0 for Au(111) (Ref. 7) and of 3.8 for Pt(111).[4]

Figure 3(a) shows a STM image of several atomic terraces partly covered by the second layer exhibiting the domain-wall network in coexistence with terraces covered by the flat imaged first layer. In the middle of the image there is a Ag (1×1) terrace that exhibits two worm-shaped depletions running almost vertical. They exceed from the connection to the second layer over 100 Å into the terrace. Comparison with the orientation of the domain walls shows that they run along the [11$\bar{2}$] direction. These linear depletions are never found for submonolayer coverages and are always restricted to the area where the first and the second layer grown on the underlying Pt terrace touch each other on the same atomic level. They can be considered as a localized restructuring of the first layer, which has been induced by the presence of the second layer. Due to the equal imaging height of these linear depletions with domain walls from the network, they have to be areas of locally reduced Ag atom density. However, their structure cannot be the one of simple domain walls because they do not separate fcc and hcp stacking areas. Presumably the structure inside these stripes is similar to two adjacent domain walls from the SI phase described above.

Growing thicker films, the symmetry changes slowly

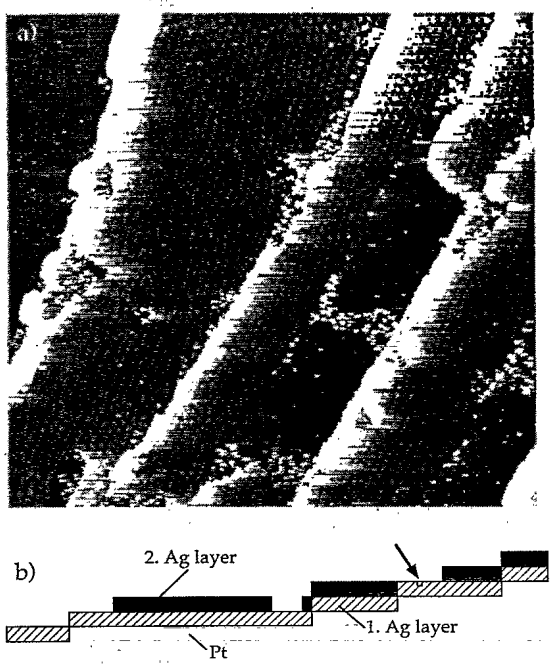

FIG. 3. (a) STM image showing that the flat imaged (1×1) Ag layer has dark imaged linear stripes which are local dilutions induced by the domain-wall network (Θ=1.5 ML, T_a=800 K, 2500×2500 Å^2). (b) Schematic profile showing the stacking of atomic layers in a horizontal cut at the arrows in (a).

from trigonal to hexagonal. This change in symmetry is in accordance with observations from He diffraction.[16] STM images of the third monolayer (not shown here), for example, exhibit a periodic structure consisting of hexagonally arranged protruding areas surrounded by darker lines which separate them from a homogeneously protruding area. The orientation of the unit cell characterizing this structure is rotated by 30° against the one of the second layer. The structure is by far less regular than the trigonal network of the bilayer. However, the images show that the third layer is still incommensurate and has a nonisotropic stress tensor.

The metastable SI phase formed by the unannealed second Ag layer is generally found for many weakly incommensurate phases. Examples are the Au(111) reconstruction and the striped phase for the Cu/Ru(0001) system.[11] The Pt(111) reconstruction is also an example, when the atomic structure of the domain walls and their pairwise arrangement is considered.[5] In all these examples the topmost layers reveal a higher density compared to the underlying bulk, which involves domain walls with a locally increased density. In our case, the atomic density is locally reduced at the domain walls, which has the structural consequence that they are narrower and implies a lower quantity of unfavorable adsorption sites. The fact that this structure is metastable is due to its restriction to locally unidirectional strain relief. In the case of Au, Pt, and Cu/Ru(0001) this handicap is overcome by alteration of the direction with the highest strain. For these systems this seems to be the only way to a more isotropic strain relief. The SI phase is stable for Cu/Ru(0001) upon annealing to 1000 K, Au(111) reveals this phase up to 880 K,[17] and the structure imaged by Bott *et al.* for Pt(111) is considered to be very similar to the high-temperature reconstruction. Thus the domain-wall interaction energy seems to be too high to allow for domain-wall crossing. This can be caused by on-top adsorption sites, which would have to be involved in these crossing points.[18] In our case domain walls are diluted zones which apparently have a lower interaction energy. In particular, they do not involve unfavorable sites at their crossing points. This makes it reasonable that a trigonal domain-wall network can be established upon annealing, which allows for an isotropic strain relief on a more local scale. Interestingly very similar networks are formed, e.g., in surfactant mediated growth of Ge on Si(111),[19] for Na adsorption on Au(111),[20] and for the β phase of Ga on Ge(111).[21] In all these cases the systems try to increase their fraction of ideal stacking with respect to the faulted one. For Na/Au(111) and Ga/Ge(111) the domain walls are crossing in one point. In the alkali-metal case, therefore, the domain walls bend and thus incline alternating smaller (hcp) and bigger (fcc) triangles. In the latter case, the domain walls have different width [see Fig. 2(b)], which allows for bigger fcc areas. In the Ag/Pt(111) case, the introduction of a phase shift allows for each fraction of fcc to hcp stacking between 1 (offset δ=0) and 3 (δ=0.5a). The further advantage of this phase shift is that crossing of all three domain walls is avoided.

[1]A. D. Novaco and J. P. McTague, Phys. Rev. Lett. **38**, 1286 (1977).
[2]J. Perdereau *et al.*, J. Phys. F **4**, 798 (1974).
[3]Y. Tanishiro *et al.*, Surf. Sci. **111**, 395 (1981).
[4]A. R. Sandy *et al.*, Phys. Rev. Lett. **68**, 2192 (1992).
[5]M. Bott *et al.*, Phys. Rev. Lett. **70**, 1489 (1993).
[6]U. Harten *et al.*, Phys. Rev. Lett. **54**, 2619 (1985).
[7]J. V. Barth *et al.*, Phys. Rev. B **42**, 9307 (1990).
[8]S. Narasimhan and D. Vanderbilt, Phys. Rev. Lett. **69**, 1564 (1992).
[9]H. Röder, H. Brune, J. P. Bucher, and K. Kern, Surf. Sci. **298**, 121 (1993).
[10]H. Röder *et al.*, Phys. Rev. Lett. **71**, 2086 (1993).
[11]G. O. Pötschke and R. J. Behm, Phys. Rev. B **44**, 1442 (1991).
[12]Y. Okwamoto and K. H. Bennemann, Surf. Sci. **186**, 511 (1987).
[13]P. Bak *et al.*, Phys. Rev. B **19**, 1610 (1979).
[14]J. Tersoff and D. R. Hamann, Phys. Rev. B **31**, 805 (1985).
[15]J. Schröder *et al.*, Ultramicroscopy **42-44**, 475 (1992).
[16]B. Poelsema (private communication).
[17]A. R. Sandy *et al.*, Phys. Rev. B **43**, 4667 (1991).
[18]The Pt(111) reconstruction can already be seen as the intermediate case, because it reveals one type of "star" where six domain walls meet in one point, thus domain-wall crossing occurs. However, the fact that this is avoided in the other type of stars and the low density of crossing points shows that crossing is unfavorable for this surface.
[19]M. Horn-von-Hoegen, A. A. Falou, H. Pietsch, B. H. Müller, and M. Henzler, Surf. Sci. **298**, 29 (1993).
[20]J. V. Barth, R. J. Behm, and G. Ertl (unpublished).
[21]M. Böhringer (private communication).